Solutions Classification
to the Extended Reduced Ostrovsky Equation

Yury A. STEPANYANTS

Australian Nuclear Science and Technology,
Organisation PMB 1, Menai (Sydney), NSW, 2234, Australia
E-mail: *yuas50@gmail.com*

Abstract. An alternative to the Parkes' approach [*SIGMA* **4** (2008), 053, 17 pages] is suggested for the solutions categorization to the extended reduced Ostrovsky equation (the exROE in Parkes' terminology). The approach is based on the application of the qualitative theory of differential equations which includes a mechanical analogy with the point particle motion in a potential field, the phase plane method, analysis of homoclinic trajectories and the like. Such an approach is seemed more vivid and free of some restrictions contained in [*SIGMA* **4** (2008), 053, 17 pages].

Key words: reduced Ostrovsky equation; mechanical analogy; phase plane; periodic waves; solitary waves, compactons

2000 Mathematics Subject Classification: 35Q58; 35Q53; 35C05

1 Introduction

In paper [1] E.J. Parkes presented a categorization of solutions of the equation dubbed the extended reduced Ostrovsky equation (exROE). The equation studied has the form

$$\frac{\partial}{\partial x}\left(\mathcal{D}^2 u + \frac{1}{2}pu^2 + \beta u\right) + q\mathcal{D}u = 0, \qquad \text{where} \quad \mathcal{D} = \frac{\partial}{\partial t} + u\frac{\partial}{\partial x} \tag{1}$$

with p, q, and β being constant coefficients. This equation was derived from the Hirota–Satsuma-type shallow water wave equation considered in [2] (for details see [1]).

For stationary solutions, i.e. solutions in the form of travelling waves depending only on one variable $\chi = x - Vt - x_0$, this equation reduces to the simple third-order ODE:

$$\frac{d}{d\chi}\left[w\frac{d}{d\chi}\left(w\frac{dw}{d\chi}\right) + \frac{1}{2}pw^2 + (pV + \beta)w\right] + qw\frac{dw}{d\chi} = 0, \tag{2}$$

where V stands for the wave speed and $w = u - V$. (Note, that in many contemporary papers including [1] authors call such solutions simply "travelling-wave solutions". Such terminology seems not good as nonstationary propagating waves also are travelling waves. The term "stationary waves" widely used earlier seems more adequate for the waves considered here.) In paper [1], equation (2) was reduced by means of a series of transformations of dependent and independent variables to an auxiliary equation whose solutions were actually categorized subject to some restrictions on the equation coefficients, viz.:

$$p + q \neq 0, \qquad qV - \beta \neq 0$$

(one more restriction on the constant of integration for that auxiliary equation, $B = 0$, was used in [1]). Under these restrictions, solutions to equation (2) were found in analytical form

and corresponding wave profiles were illustrated graphically. Among solutions obtained there are both periodic and solitary type solutions including multivalued loop periodic waves and loop-solitons.

Similar loop solutions to exROE and some other equations were earlier obtained by Ji-Bin Li [3] who came to the conclusion that loop solutions actually are compound solutions which consist of three different independent branches. These branches may be used in various combinations representing several types of stationary propagating singular waves (waves with infinite gradients). This conclusion completely coincides with the conclusion of paper [4] where a complete classification of stationary solutions of ROE was presented. ROE derived by L.A. Ostrovsky [5] in 1978 as a model for the description of long waves in a rotating ocean (see [4] and references therein) can be treated as a particular case of exROE with $p = q$ and $\beta = 0$ (see [1]).

Below an analysis of stationary solutions to equation (2) is presented by the direct method avoiding any redundant transformations of variables. The method used is based on the phase plane concept and analogy of the equation studied with the Newtonian equation for the point particle in a potential field. Such approach seems more vivid and free of aforementioned restrictions. This work can be considered also as complementary to paper [1] as the analysis presented may be helpful in the understanding of basic properties of stationary solutions of equation (2).

2   Mechanical analogy, potential function and phase-plane method

Equation (2) can be integrated once resulting in

$$w\frac{d}{d\chi}\left(w\frac{dw}{d\chi}\right) + \frac{1}{2}(p+q)w^2 + (pV + \beta)w = C_1, \tag{3}$$

where C_1 is a constant of integration. By multiplying this equation by $dw/d\chi$ and integrating once again, the equation can be reduced to the form of energy conservation for a point particle of unit mass moving in the potential field $P(w)$:

$$\frac{1}{2}\left(\frac{dw}{d\chi}\right)^2 + P(w) = E, \tag{4}$$

where the effective "potential energy" as a function of "displacement" w is

$$P(w) = \frac{p+q}{6}w - \frac{C_1}{w} - \frac{C_2}{w^2}, \tag{5}$$

and C_2 is another constant of integration. The constant $E = -(pV + \beta)/2$ plays a role of the total energy of the particle, i.e. the sum of the "kinetic energy", $K = (1/2)(dw/d\chi)^2$, and the "potential energy", $P(w)$. As follows from equation (4), real solutions can exist only for $E \geq P(w)$. Various cases of the potential function (5) are considered below and corresponding bounded solutions are constructed. Unbounded solutions are not considered in this paper as they are less interesting from the physical point of view; nevertheless, their qualitative behavior becomes clear from the general view of corresponding phase portraits.

3   Particular case: $p + q = 0$

Consider first a particular case when the coefficients in equation (1) are such that $p + q = 0$. Note, this is one of the cases which were omitted from the consideration in paper [1]. The
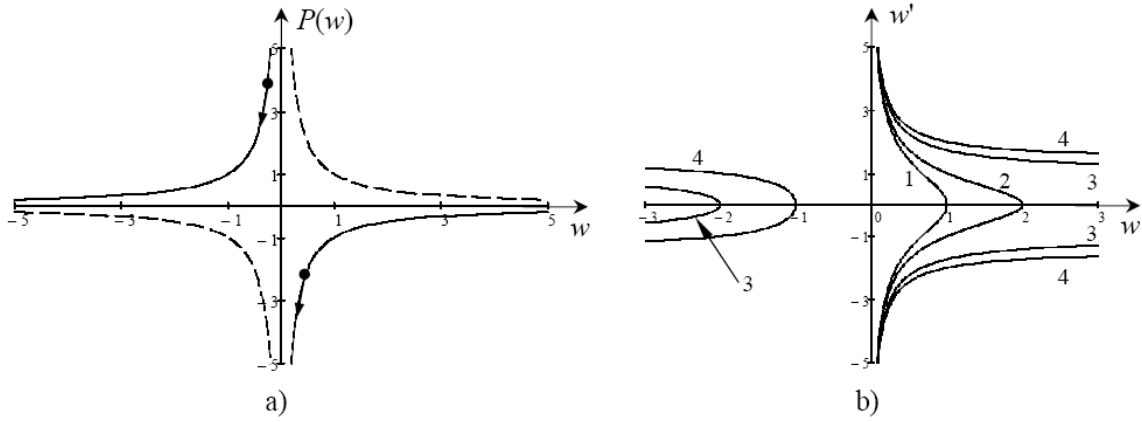
Figure 1. a) Potential function for the case $p+q=0$, $C_2=0$ and two values of C_1: $C_1=1$ (solid lines), and $C_1=-1$ (dashed lines). Two dots illustrate possible motions of point particles in the potential field. b) Phase plane corresponding to the potential function with $C_1=1$ and different values of E. Line 1: $E=-1$; line 2: $E=-0.5$; lines 3: $E=0.5$; lines 4: $E=1$.

potential function (5) simplifies in this case. However, a variety of subcases can be distinguished nevertheless even in this case depending on the coefficients C_1 and C_2. All these subcases are studied in detail below.

3a. If $C_2=0$, the potential function represents a set of antisymmetric hyperbolas located either in the first and third quadrants or in the second and fourth quadrants as shown in Fig. 1a. The corresponding phase plane (w,w'), where $w'=dw/d\chi$, is shown in Fig. 1b for $C_1=1$ (for $C_1=-1$ the phase plane is mirror symmetrical with respect to the vertical axis). For other values of C_1 phase portraits are qualitatively similar to that shown in Fig. 1 for $C_1=1$.

Analysis of the phase portrait shows that there are no bounded solutions for any positive E; corresponding trajectories both in the left half and right half of the phase plane go to infinity on w (see, e.g., lines 3 and 4 in Fig. 1b). Meanwhile, solutions bounded on w do exist for negative values of E (i.e. for $V>-\beta/p$), but they possess infinite derivatives when $w=0$. Consider, for instance, motion of an affix along the line 2 in Fig. 1b ($C_1=1$) from $w'=\infty$ towards the axis w where $w'=0$. The qualitative character of the motion becomes clear if we interpret it in terms of "particle coordinate" w and "particle velocity" w' treating ξ as the time. The motion originates at some "time" ξ_0 with infinite derivative and zero "particle coordinate" $w=0$. Then, the "particle coordinate" w increases to some maximum value $w_{\max}=-C_1/E$ ($E<0$) as the "particle velocity" is positive. Eventually it comes to the rest having zero derivative $w'=0$ and $w=w_{\max}$. Another independent branch of solution for the same value of E corresponds to the affix motion along the line 1 from the previously described rest point at axis w towards $w'=-\infty$ and $w=0$.

All bounded analytical solutions for this case can be presented in the universal implicit form:

$$\xi(y)-\xi_0=\pm\left[\arctan\left(\sqrt{\frac{y}{1-y}}\right)-\sqrt{y(1-y)}\right],\tag{6}$$

where $y=-Ew/C_1$, $\xi=-\sqrt{2}(-E)^{3/2}\chi/C_1$ and ξ_0 is an arbitrary constant of integration. This solution consists of two independent branches which correspond to signs plus or minus in front of the square brackets in equation (6). Each branch is defined only on a compact support of axis ξ: either on $-\pi/2\le\xi-\xi_0\le0$ or on $0\le\xi-\xi_0\le\pi/2$ (see lines 1 and 1′ in Fig. 2). With the appropriate choice of constants ξ_0 one can create a variety of different solutions, e.g., the V-shape wave (see lines 2 and 2′), or a smooth-crest compacton, i.e. a compound solitary wave defined only for $|\xi-\xi_0|\le\pi/2$ (see lines 3 and 3′). Using a translational invariance of
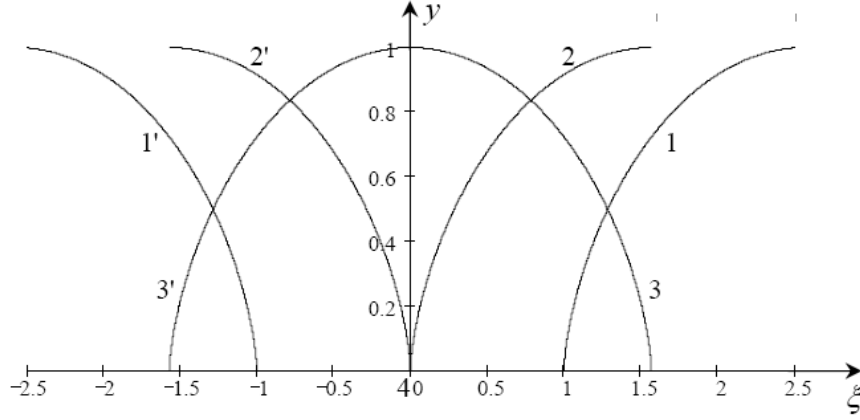
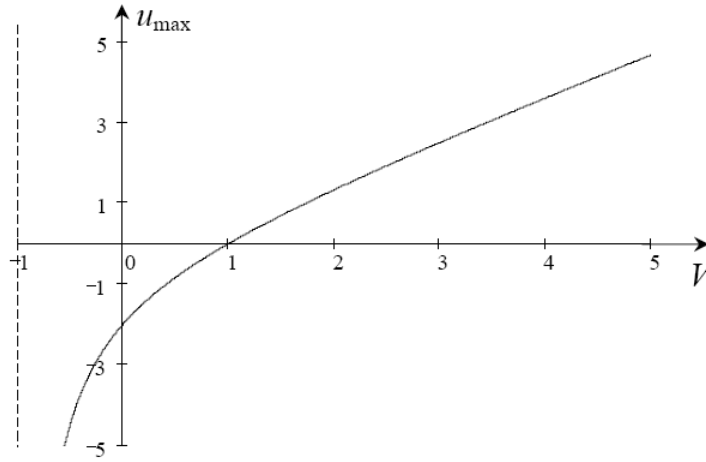**Figure 2.** Various particular solutions described by equation (6).

Figure 3. Maximum of the compacton solution (6) against speed in the original variables, equation (7). Dashed vertical line corresponds to the limiting value of $V = -\beta/p$. The plot is generated for $C_1 = p = \beta = 1$.

solutions and their independency of each other, one can create periodic or even chaotic sequences of compactons randomly located on axis ξ.

The maximum of the function $y(\xi)$, $y_{\max} = 1$, corresponds in terms of w to $w_{\max} = -C_1/E$. Using the relationship between w and the original variable u (see above), as well as the definition of the constant E, one can deduce the relationship between the wave extreme value (wave maximum) and its speed:

$$u_{\max} = V - \frac{C_1}{E} = V + \frac{2C_1}{pV + \beta}. \tag{7}$$

Taking into account that we consider the case of $C_1 = 1$, and negative values of E are possible only when $V > -\beta/p$, the plot of $u_{\max}(V)$ is such as presented in Fig. 3.

As follows from equation (7), a wave is entirely negative ($u_{\max} < 0$), when

$$V < \frac{1}{2p}\left(\sqrt{\beta^2 - 8pC_1} - \beta\right),$$

provided that $p < \beta^2/(8C_1)$. At greater values of V, the wave profile contains both positive and negative pieces, and for certain value of V the total wave "mass" $I = \int u(\chi)d\chi$ vanishes (the integral here is taken over the entire domain where function $u(\chi)$ is defined).
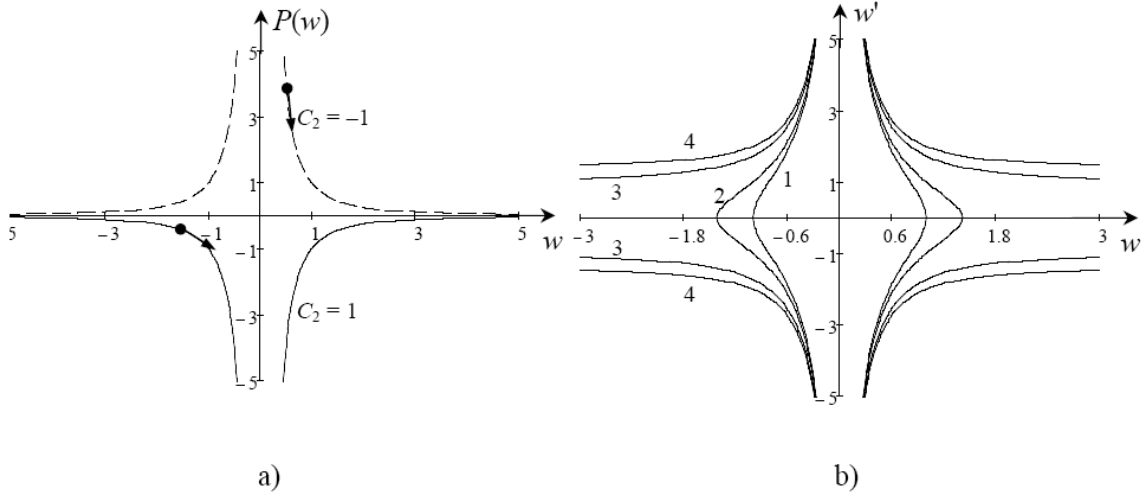
a)   b)

Figure 4. a) Potential function for the case $p+q = 0$, $C_1 = 0$ and two values of C_2: $C_2 = 1$ (solid lines), and $C_2 = -1$ (dashed lines). Two dots illustrate possible motions of point particles in the potential field. b) Phase plane corresponding to the potential function with $C_2 = 1$ and different values of E. Line 1: $E = -1$; line 2: $E = -0.5$; lines 3: $E = 0.5$; lines 4: $E = 1$. All lines are symmetrical with respect to axis w' and are labelled only in the left half of the phase plane.

3b. A similar analysis can be carried out for the case when $C_1 = 0$, $C_2 \neq 0$. The potential function in this case represents a set of symmetric quadratic hyperbolas located either in the first and second quadrants or in the third and fourth quadrants as shown in Fig. 4a for $C_2 = \pm 1$. The corresponding phase plane is shown in Fig. 4b for $C_2 = 1$ only (there are no bounded solutions for $C_2 = -1$, therefore this case is not considered here). For other positive values of C_2 phase portraits are qualitatively similar to that shown in Fig. 4b.

Analysis of the phase portrait shows that there are no bounded solutions for $C_2 = -1$, as well as for $C_2 = 1$ and any positive E (see, e.g., lines 3 and 4 in Fig. 4b); they exist however for $C_2 = 1$ and negative values of E, but possess infinite derivatives at some values of χ. In normalized variables $y = (-E/C_2)^{1/2}w$, $\xi = -E(2/C_2)^{1/2}\chi$ all possible solutions can be presented in terms of independently chosen function branches describing a unit circle in one of the four quadrants, i.e.

$$(\xi - \xi_0)^2 + y^2 = 1, \tag{8}$$

where ξ_0 is an arbitrary constant of integration.

Playing with the constant ξ_0 one can create again a variety of compacton-type solutions including multi-valued solutions. Some examples of solitary compacton solutions are shown in Fig. 5a; they include N-shaped waves, multi-valued circle-shaped waves and semicircle positive-polarity pulses (due to symmetry, the polarity of the first and last waves can be inverted). In addition to those, various periodic and even chaotic compound waves can be easily constructed; one of the possible examples of a periodic solution is shown in Fig. 5b. Each positive or negative half-period of any wave consists of two independent branches originating at $y = 0$ and ending at $y = \pm 1$. The same is true for the pulse-type solutions shown in Fig. 5a; they consist of independent symmetrical branches as shown, for example, for the semicircle pulse in Fig. 5a where they are labelled by symbols 1 and 2.

The maximum of the function $y(\xi)$, $y_{\max} = 1$, corresponds in terms of w to the wave maximum, $w_{\max} = (-C_2/E)^{1/2}$. Using a relationship between w and the original variable u (see above), as well as definition of the constant E, one can deduce the relationship between the
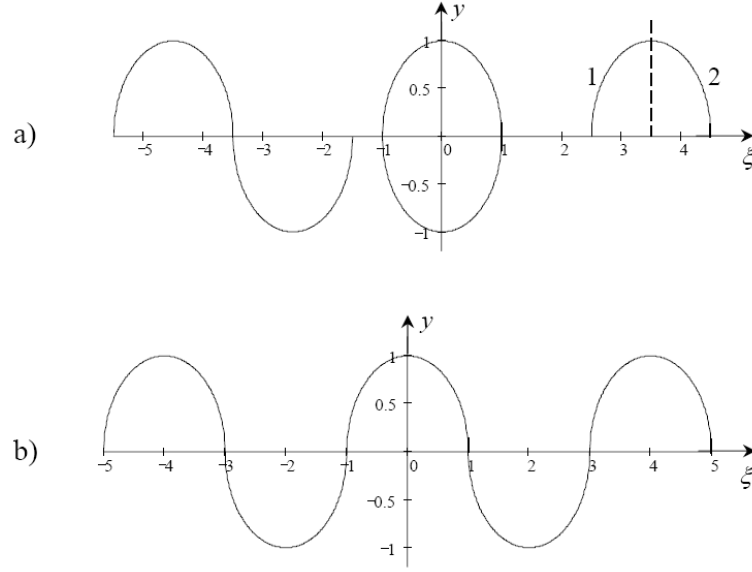
Figure 5. a) Some examples of pulse-type waves described by equation (8): N-shaped wave; circle wave and semicircle compacton. b) One of the examples of a periodic wave with infinite derivatives at $y = 0$, $\xi = 2n + 1$, where n is an entire number.

wave maximum and its speed:

$$u_{\max} = V + \sqrt{\frac{-C_2}{E}} = V + \sqrt{\frac{2C_2}{pV + \beta}}. \tag{9}$$

The plot of $u_{\max}(V)$ is presented in Fig. 6 for $V > -\beta/p$ in accordance with the chosen constant $C_2 = 1$ and $E < 0$.

As follows from equation (9), wave maximum (minimum) cannot be less than the certain value, $U_{\max}$ ($-U_{\min}$), which occurs at some speed V_1, where

$$U_{\max} = \frac{1}{p} \left[\left(\frac{C_2 p^2}{2} \right)^{1/3} - \beta \right] + 2 \left(\frac{C_2}{2p} \right)^{1/3}, \qquad V_1 = \frac{1}{p} \left[\left(\frac{C_2 p^2}{2} \right)^{1/3} - \beta \right].$$

For all possible values of wave maximum $u_{\max} > U_{\max}$, two values of wave speed are possible, i.e. two waves of the very same "amplitude" can propagate with different speeds. This is illustrated by horizontal dashed line in Fig. 6 drawn for $u_{\max} = 2.5$. The same is true for waves of negative polarity.

3c. Consider now the case when both C_1 and C_2 are nonzero but $p + q$ is still zero. There are in general four possible combinations of signs of the parameters C_1 and C_2:

i) $C_1 > 0$, $C_2 > 0$;   ii) $C_1 < 0$, $C_2 > 0$;   iii) $C_1 > 0$, $C_2 < 0$;   iv) $C_1 < 0$, $C_2 < 0$.

The shape of the potential function $P(w)$ and corresponding solutions are different for all these cases. However, among them there are only two qualitatively different and independent cases, whereas the two others can be obtained from those two cases using simple symmetry reasons. This statement is illustrated by Fig. 7, where the potential relief is shown for all four aforementioned cases i)–iv).

As one can see from Fig. 7, cases i) and ii), as well as iii) and iv), are mirror symmetrical counterparts of each other with respect to the vertical axis. This implies that solutions for the cases i) and ii), and correspondingly, iii) and iv), are related by the simple sign interchange
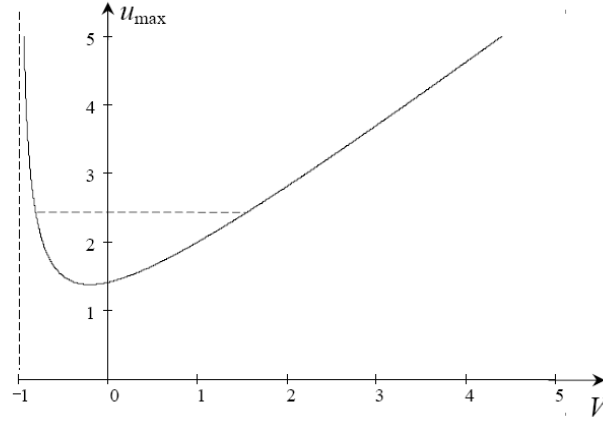
Figure 6. Dependence of the wave maximum on speed in original variables, equation (9), as follows from solution (8). Dashed vertical line corresponds to $V = -\beta/p$. The plot is generated for $C_2 = p = \beta = 1$.
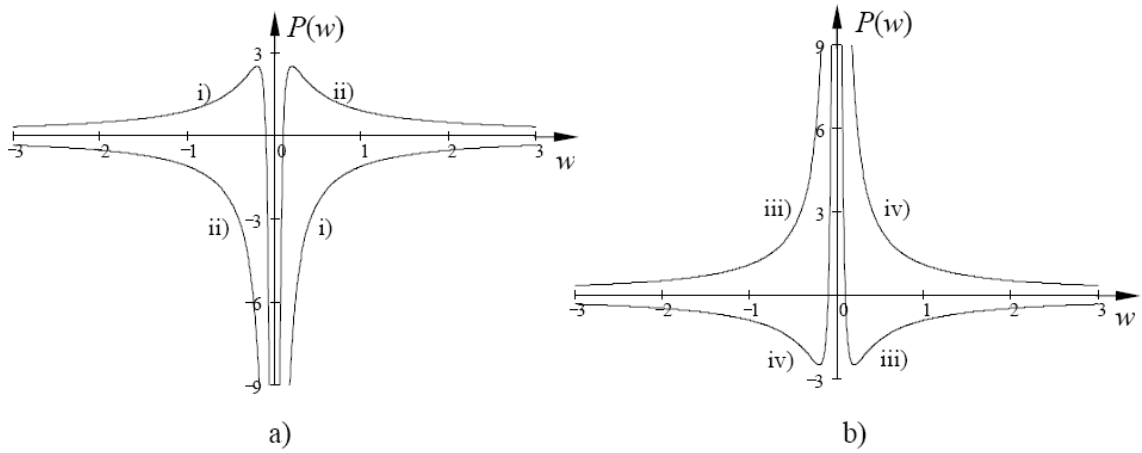

Figure 7. Potential relief for the four different cases, i)–iv), of various signs of constants C_1 and C_2. The plot was generated for $C_1 = \pm 1$, $C_2 = \pm 0.1$.

operation, i.e. $w_{\text{i}} = -w_{\text{ii}}$, $w_{\text{iii}} = -w_{\text{iv}}$. Therefore, below only two qualitatively different cases are considered in detail, namely the cases i) and iii).

Case i) is characterized by an infinite potential well at the origin, $w = 0$. This singularity in the potential function corresponds to the existence of a singular straight line $w = 0$ on the phase plane (see Fig. 8). On both sides from this singular line there are qualitatively similar trajectories which correspond to bounded solutions having infinite derivatives at the edges. Quantitative difference between the "left-hand side solutions" and "right-hand side solutions", apart of their different polarity, is the former solutions (of negative polarity, $w \leq 0$) exist for $E \leq P_{\max}$, whereas the latter ones (of positive polarity, $w \geq 0$) exist for $E \leq 0$. The potential function has a maximum $P_{\max} = C_1^2/(4C_2)$ at $w = -2C_2/C_1$. There are no bounded solutions for $E > P_{\max}$.

Consider first bounded solutions which correspond to trajectories shown in the left half-plane, $w \leq 0$, in Fig. 8. For a positive value of the parameter E in the range $0 \leq E \leq P_{\max}$, the analytical solution can be presented in the form

$$\xi(y) = \pm 2\sqrt{Q}\left[\sqrt{(y+2Q)^2 - 4Q(Q-1)} - 2Q\ln\frac{y+2Q+\sqrt{(y+2Q)^2 - 4Q(Q-1)}}{2\sqrt{Q(Q-1)}}\right], \quad (10)$$

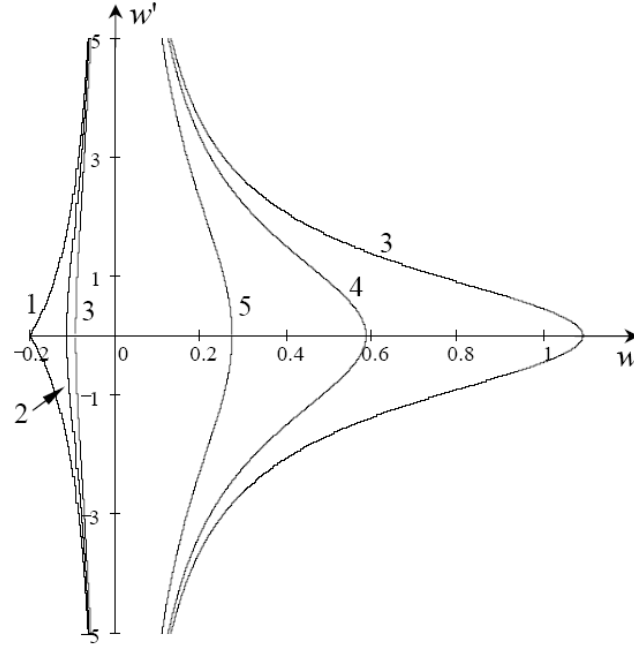where $\xi = \chi\sqrt{2C_2}(C_1/C_2)^2$, $y = w(C_1/C_2)$, $Q = C_1^2/(4C_2E)$.

Figure 8. Phase portrait of equations (3), (4) for the case i) (only those trajectories are shown which correspond to particle motion within the potential well in Fig. 7a). Line 1: $E = 2.5$; line 2: $E = 1$; lines 3: $E = -1$; line 4: $E = -2$; line 4: $E = -5$.

The range of variability on ξ is:

$$|\xi| \le 4Q \left\{ 1 - \sqrt{Q} \ln \left[(\sqrt{Q} + 1)/\sqrt{Q - 1} \right] \right\},$$

whereas y varies in the range

$$-2 \left[Q - \sqrt{Q(Q - 1)} \right] \le y \le 0.$$

The relationship between the wave minimum and its speed is:

$$u_{\min} = V + \frac{C_1}{pV + \beta} + \sqrt{\frac{2C_2}{pV + \beta} \left[\frac{C_1^2}{2C_2(pV + \beta)} + 1 \right]}, \tag{11}$$

where $pV + \beta < 0$ as $E > 0$.

If $E < 0$, then the solution is

$$\xi(y) = \pm 2\sqrt{-Q} \left[\sqrt{4Q(Q - 1) - (y + 2Q)^2} \right.$$

$$\left. + 2Q \arctan \left(\frac{y + 2Q}{\sqrt{4Q(Q - 1) - (y + 2Q)^2}} \right) + \pi Q \right]. \tag{12}$$

The range of variability on ξ is: $|\xi| \le -4Q \left[1 + \sqrt{-Q} \left(\arctan \sqrt{-Q} - \pi/2 \right) \right]$, whereas y varies in the range $-2 \left[Q + \sqrt{Q(Q - 1)} \right] \le y \le 0$. The relationship between the wave minimum and its speed is also given by equation (11), but with $pV + \beta > 0$.

Two special cases of solution (10) can be mentioned. When $Q = 1$ ($E = P_{\max}$), solution (10) with the appropriate choice of the integration constant reduces to

$$\xi(y) = \pm 4 \left[\frac{y}{2} - \ln \left(1 + \frac{y}{2} \right) \right]. \tag{13}$$

This solution is unbounded on ξ, i.e. it is defined in the range: $|\xi| \leq \infty$. However, the solution is bounded on y: $-2 \leq y \leq 0$. The relationship between the wave minimum and its speed is simple as both of them are constant values in this special case:

$$V = -\frac{1}{p}\left(\beta + \frac{C_1^2}{2C_2}\right), \qquad u_{\min} = V - 2\frac{C_2}{C_1} = -\frac{1}{p}\left(\beta + \frac{C_1^2}{2C_2} + 2p\frac{C_2}{C_1}\right). \tag{14}$$

Another special case corresponds to $Q = \infty$ ($E = 0$); in this case equation (10) after appropriate choice of integration constant reduces to:

$$\xi(y) = \pm\frac{2}{3}\sqrt{y+1}(y-2). \tag{15}$$

The range of variability on ξ is: $|\xi| \leq 4/3$, whereas y varies in the range: $-1 \leq y \leq 0$. The relationship between the wave minimum and its speed is also very simple as both of them are again constants but different from those given by equation (14); in this case they are:

$$V = -\frac{\beta}{p}, \qquad u_{\min} = V - \frac{C_2}{C_1} = -\left(\frac{\beta}{p} + \frac{C_2}{C_1}\right).$$

Bounded solutions corresponding to the trajectories shown in the right half-plane in Fig. 8 with $w \geq 0$, exist only for negative E; they are given by equation (12), but with the different range of variability of y: $0 \leq y \leq 2\left[-Q + \sqrt{Q(Q-1)}\right]$. The relationship between the wave maximum and its speed is given again by equation (11) where $u_{\max}$ should be substituted instead of $u_{\min}$ and $pV + \beta > 0$ as $E < 0$ for these solutions.

Solutions (10), (12), (13) and (15) are shown in Fig. 9. All these solutions are of the compacton type; they consist of two independent branches which can be matched differently or unmatched at all. Lines 2 and 2′ represent an example when two branches are matched so that they form a semi-oval; lines 3 and 3′ represent another example when two branches are matched so that they form an inverted "seagull". On the basis of these "elementary" solutions, various complex compound solutions can be constructed including periodic or chaotic stationary waves.

The dashed line 1 in the figure corresponds to $E = 0$ ($Q = 8$). Another branch of the solution with the same value of $E = 0$ represents a solution of positive polarity which is unbounded both on ξ and y. For positive values of E, solutions of negative polarity become wider and of greater "amplitude" (see line 2). When E further increases and approaches $P_{\max}$, the solution becomes infinitely wide, but its minimum goes to -2. In the limiting case $E = P_{\max}$ ($Q = 1$) two independent branches of the solution can be matched differently as shown by dashed-dotted lines 3 and 3′ in Fig. 9. The solution vanishes in this case when $\xi = 0$ and goes to -2 when $\xi \to \pm\infty$; this situation is described by equation (13).

For the negative E there are two families of solutions: negative one, corresponding to the left-hand side trajectories in Fig. 8, and positive one, corresponding to the right-hand side trajectories. When E, being negative, increases in absolute value (Q varies from $-\infty$ to 0_-), solutions depart from the line 1 in Fig. 9 and gradually squeeze to the origin (see line 4 for instance). For the same values of negative E, positive solutions originated at infinity also gradually shrink and collapse in the origin (lines 6 and 5 demonstrate this tendency).

Consider now the case iii) shown in Fig. 7b. The potential function in this case has only one well of a finite depth so that $P_{\min} = C_1^2/(4C_2)$ at $w = -2C_2/C_1$, where C_2 is negative now. There are no bounded solutions for negative w; they exist however for positive w and E varying in the range $P_{\min} \leq E < 0$. The finite value of the potential minimum corresponds to the equilibrium point of the centre type in the phase plane. There is also a family of closed trajectories for the above indicated range of E variation (see Fig. 10); these trajectories correspond to periodic solutions.
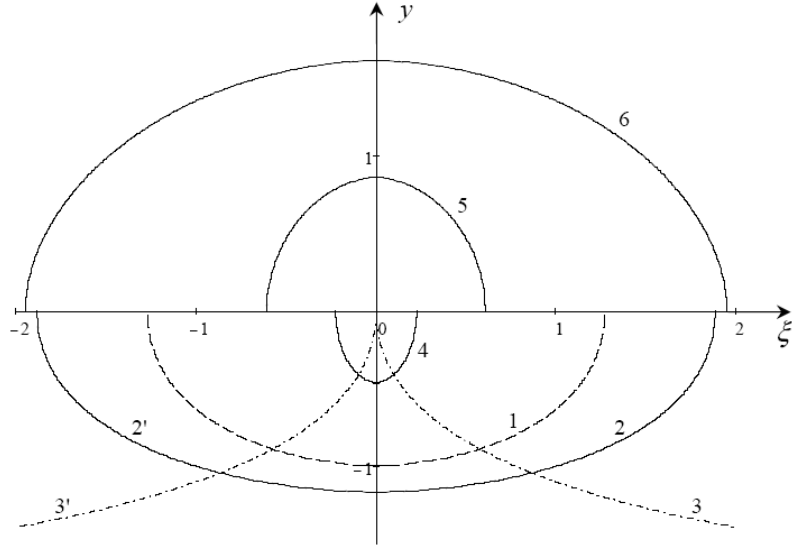
Figure 9. Various solutions described by equations (10), (12), (13) and (15). Compactons of negative polarity: line 1: $Q = \infty$; lines 2 and 2': $Q = 2$; lines 3 and 3': $Q = 1$: line 4: $Q = -0.1$. Compactons of positive polarity: line 5: $Q = -0.1$; line 6: $Q = -0.25$.
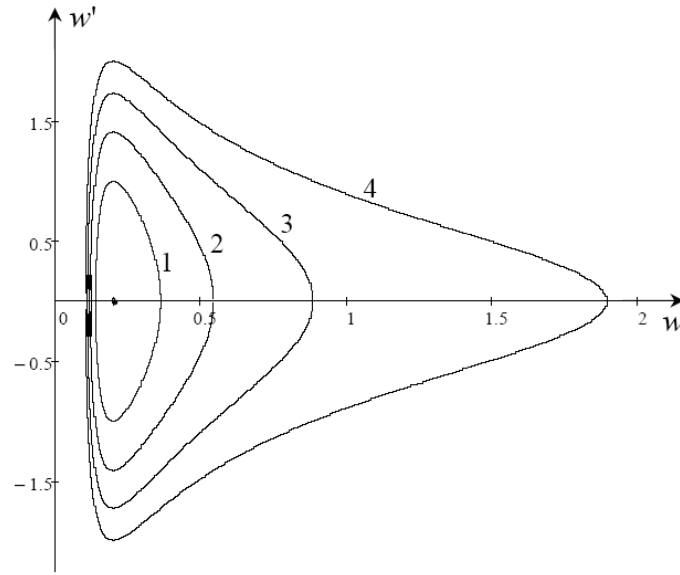

Figure 10. Phase portrait of equations (3), (4) for the case **3c** iii) (only those trajectories are shown which correspond to particle motion within the potential well in Fig. 7b). The dot at the center of closed lines indicates an equilibrium point corresponding to the potential minimum ($E = -2.5$ for the chosen set of parameters: $C_1 = 1$, $C_2 = -0.1$); line 1: $E = -2$; line 2: $E = -1.5$; line 3: $E = -1$; line 4: $E = -0.5$.

As usual, closed trajectories around the center ($E \geq P_{\min}$) correspond to quasi-sinusoidal solutions. Whereas other closed trajectories ($E > P_{\min}$) correspond to non-sinusoidal periodic waves with smooth crests and sharp narrow troughs. The larger is the value of E, the longer is the wave period. The period tends to infinity when $E \to 0_-$. The analytical form of this family of solutions is described by the following equation:

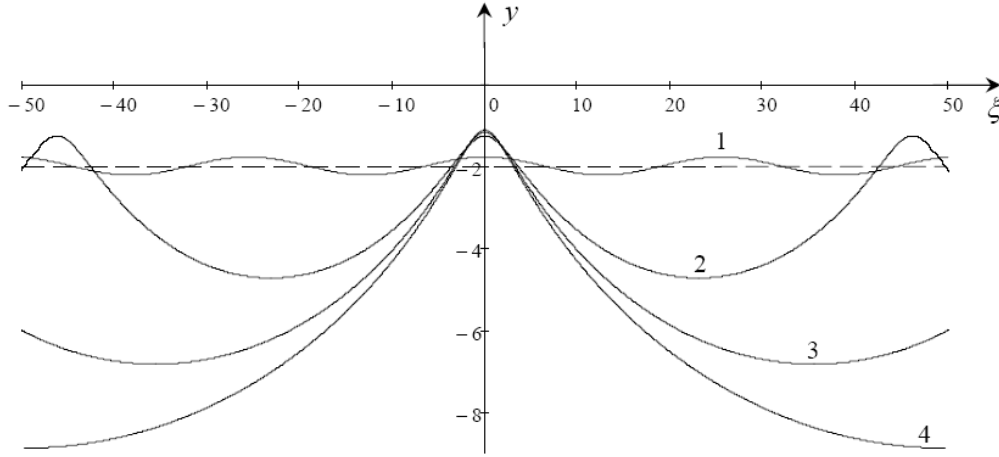$$\xi(y) = \pm 2\sqrt{Q}\left[\sqrt{4Q(Q-1) - (y + 2Q)^2}\right.$$

Figure 11. Various solutions described by equation (16). Line 1 (quasi-sinusoidal wave): $Q = 1.01$; line 2: $Q = 1.5$; line 3: $Q = 2$; line 4: $Q = 2.5$. Dashed lines shows the equilibrium state $y = -2$.

$$+ 2Q \arctan \left(\frac{y + 2Q}{\sqrt{4Q(Q-1) - (y + 2Q)^2}} \right) - \pi Q \Bigg], \tag{16}$$

where $\xi = \chi \sqrt{-2C_2}(C_1/C_2)^2$, $y = w(C_1/C_2)$, $Q = C_1^2/(4C_2 E)$. Solution (16) is shown in Fig. 11 for different values of Q (note that the solution is negative in terms of y because $C_2 < 0$). As follows from equation (16), y varies in the range:

$$-2 \left[Q + \sqrt{Q(Q-1)} \right] \le y \le -2 \left[Q - \sqrt{Q(Q-1)} \right],$$

whereas the dependence of wave period Λ on Q is: $\Lambda(Q) = 8\pi Q\sqrt{Q}$. The wave period varies from 8π to infinity when Q increases from unity to infinity.

From the extreme values of y (see above indicated range of its variability) one can deduce the dependences of wave maximum and minimum on speed in the original variables. The corresponding formulae are:

$$u_{\max,\min}(V) = V + \frac{C_1}{pV + \beta} \mp 2C_2 \sqrt{\frac{1}{2C_2(pV + \beta)} \left[\frac{C_1^2}{2C_2(pV + \beta)} + 1 \right]}, \tag{17}$$

where the upper sign in front of the root corresponds to the wave maximum and lower sign – to the wave minimum. These dependences are plotted in Fig. 12 for $V > -\beta/p$ in accordance with the chosen values of constants $C_1 = 1$, $C_2 = -0.1$ and $E < 0$. The asymptote $V = -\beta/p$ is shown in the figure by the vertical dashed line. As follows from equation (15), wave maximum cannot be less than the certain value, $U_{\max}$, which occurs at some speed V_1 shown in Fig. 12.

For all possible values of wave maximum $u_{\max} > U_{\max}$, two values of wave speed are possible, i.e. two periodic waves of the same maximum (but not minimum!) can propagate with different speeds. This is illustrated by the horizontal dashed line shown in Fig. 12 and drawn for $u_{\max} = 2.5$. In original variables quasi-sinusoidal waves exist when the speed is close to its limiting value $V_{\max} = -\frac{1}{p} \left(\frac{C_1^2}{2C_2} + \beta \right)$; there are no waves with greater speed. When $V \le V_{\max}$, the wave minimum and maximum are close to each other. Then, when the speed decreases, the gap between wave maximum and minimum gradually increases and goes to infinity when the speed approaches its minimum value $V_{\min} = -\beta/p$.
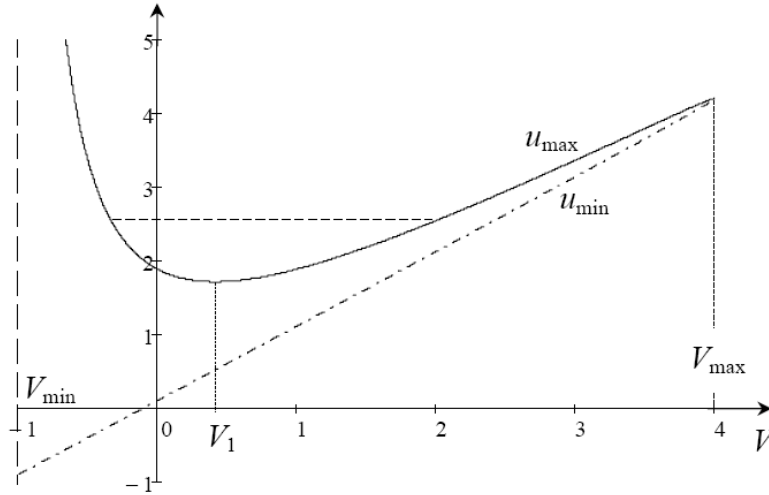
Figure 12. Dependences of wave maximum (solid line) and minimum (dashed-dotted line) on speed in the original variables, equation (17), as follows from the solution (16). Dashed vertical line corresponds to $V = -\beta/p$. The plot is generated for $C_1 = 1$, $C_2 = -0.1$ and $p = \beta = 1$.

4   General case: $p + q \neq 0$

Consider now a more general case when the coefficients in equation (1) are such that $p + q \neq 0$. The basic equation (4) can be presented in the new variables $\eta = (p+q)\chi/6$ and $v = (p+q)w/6$ with the same constant of integration $E = -(pV + \beta)/2$, but with new effective potential function

$$P(v) = v - \frac{C_1}{v} - \frac{C_2}{v^2}. \tag{18}$$

The potential function is monotonic when $C_1 = C_2 = 0$, and there are no bounded solutions in this case. Bounded solutions may exist if at least one of these constants is nonzero. Below we present possible forms of the potential function and corresponding phase portraits of bounded solutions for various relationships between constants C_1 and C_2. Qualitatively all these cases are similar to those which have been described already in the previous section, therefore we omit the detailed analysis and do not present analytical solutions as they can be obtained straightforwardly and expressed in terms of elliptic functions.

4a. If $C_2 = 0$, the potential function represents a set of antisymmetric hyperbolas located either in the first and third quadrants when $C_1 = -1$, or in the second and fourth quadrants when $C_1 = 1$; this is shown in Fig. 13.

For the case of $C_1 = 1$ only bounded solutions of a compacton type are possible for positive v. Such solutions correspond to the motion of particle c shown in the figure down to the potential well. This family of pulse-type solutions exist both for negative and positive E; all of them are bounded from the top with the maximum values depending on E, have zero minimum values and infinite derivatives when $v = 0$. Corresponding phase plane is presented in Fig. 14a.

For the case of $C_1 = -1$ there are two possibilities: i) there is a family of compacton-type solutions with $v \leq 0$; they correspond to the motion of the particle b down to the potential well (particle motion to the left from the top of the "hill" corresponds to unbounded solutions). Possible values of particle energy E vary for such motions from minus infinity to $P_{\max} = -2\sqrt{-C_1}$, where $P_{\max}$ is the local maximum of the lower branch of the potential function (see Fig. 13). The phase portrait of such motions is shown in the left half of the phase plane in Fig. 14b.

ii) Another possibility appears for the particle motion within the potential well shown in the first quadrant of Fig. 13 (see the particle a). Within this well all phase trajectories are
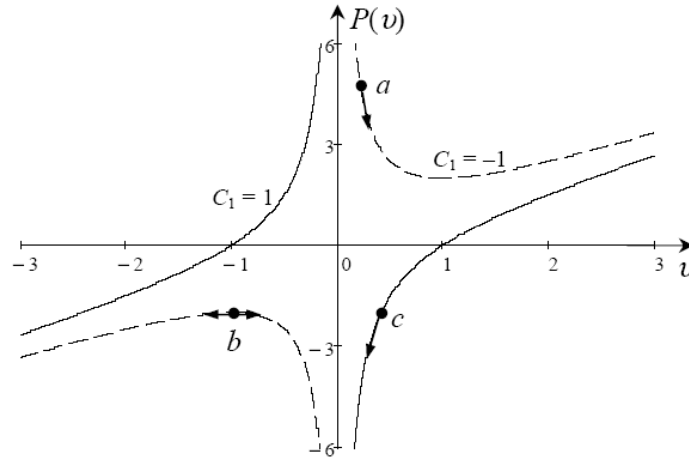
Figure 13. Potential function for the case $p + q \neq 0$, $C_2 = 0$ and two values of C_1: $C_1 = 1$ (solid line), and $C_1 = -1$ (dashed line). Dots a, b and c illustrate possible motion of a point particle in the potential field.

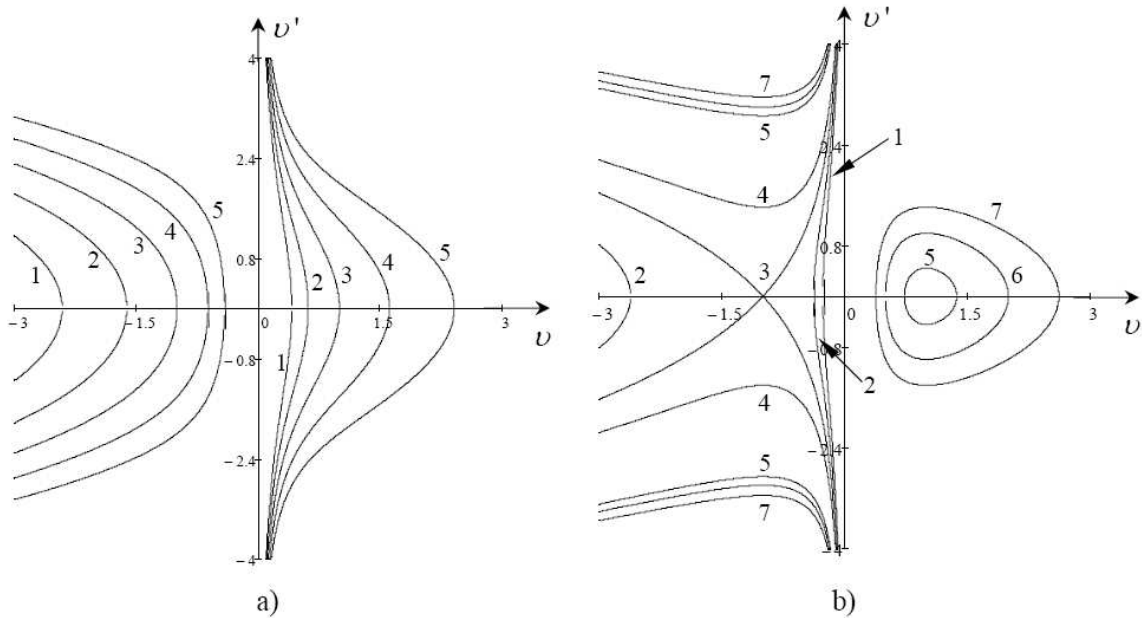a)   b)

Figure 14. a) Phase plane corresponding to the potential function with $C_1 = 1$ and various values of E. Line 1: $E = -2$; lines 2: $E = -1$; lines 3: $E = 0$; lines 4: $E = 1$; lines 5: $E = 2$. All trajectories in the left half-plane correspond to unbounded solutions. b) Phase plane corresponding to the potential function with $C_1 = -1$ and various values of E. Line 1: $E = -4$; lines 2: $E = -3$; lines 3: $E = -2$; lines 4: $E = -1$; lines 5: $E = 2.1$; lines 6: $E = 2.5$; lines 7: $E = 3$.

closed and corresponding solutions are bounded and periodical; they can be expressed in terms of elliptic functions. The phase portrait of such motions is shown in the right half of the phase plane in Fig. 14b.

4b. If $C_1 = 0$, but $C_2 \neq 0$, the potential function also represents a set of antisymmetric hyperbolas located either in the third quadrant and right half-plane in Fig. 15 when $C_2 = 1$, or in the first quadrant and left half-plane of that figure when $C_2 = -1$.

For the case of $C_2 = 1$ there are two possibilities: i) there is a family of compacton-type solutions with $v \leq 0$; they correspond to the motion of the particle b down to the potential well
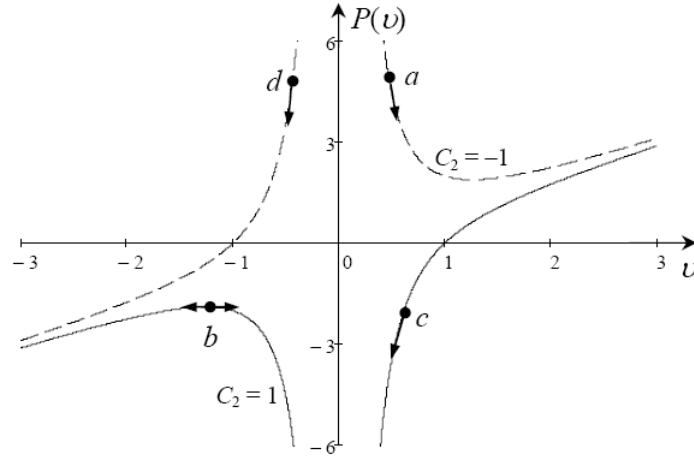
Figure 15. Potential function for the case $p + q \neq 0$, $C_1 = 0$ and two values of C_2: $C_2 = 1$ (solid lines), and $C_2 = -1$ (dashed lines). Dots a, b, c and d illustrate possible motion of a point particle in the potential field.
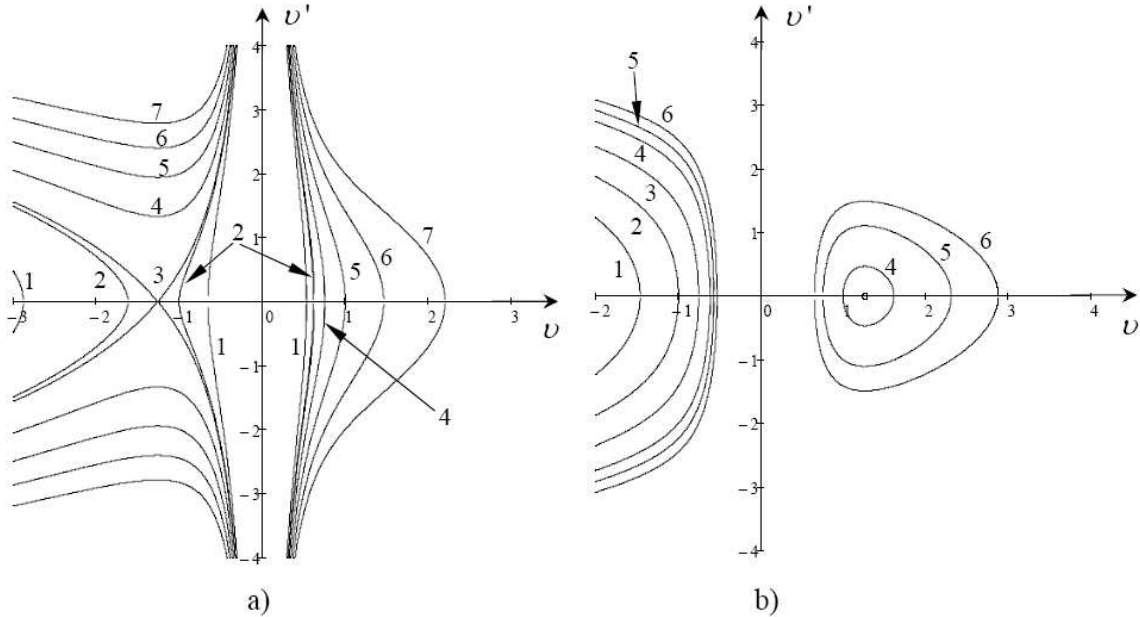

Figure 16. Phase plane corresponding to the potential function (18) with $C_1 = 0$. a) $C_2 = 1$ and various values of E. Lines 1: $E = -3$; lines 2: $E = -2$; lines 3: $E = -1.89$; lines 4: $E = -1$; lines 5: $E = 0$; lines 6: $E = 1$; lines 7: $E = 2$. b) $C_2 = -1$ and various values of E. Line 1: $E = -1$; line 2: $E = 0$; line 3: $E = 1$; lines 4: $E = 2$; lines 5: $E = 2.5$; lines 6: $E = 3$. All trajectories in the left half-plane correspond to unbounded solutions.

(particle motion to the left from the top of the "hill" corresponds to unbounded solutions). Possible values of particle energy E vary for such motions from minus infinity to $P_{\max} = 3(-C_2/4)^{1/3}$, where $P_{\max}$ is the local maximum of the left branch of the potential function (see Fig. 15). The phase portrait of such motions is shown in the left half-plane in Fig. 16a.

ii) Another family of compacton-type solutions exist with $v \geq 0$; they correspond to the motion of the particle c down to the potential well. Possible values of particle energy E for such motions vary from minus to plus infinity. Corresponding phase plane is presented in the right half-plane in Fig. 16a.
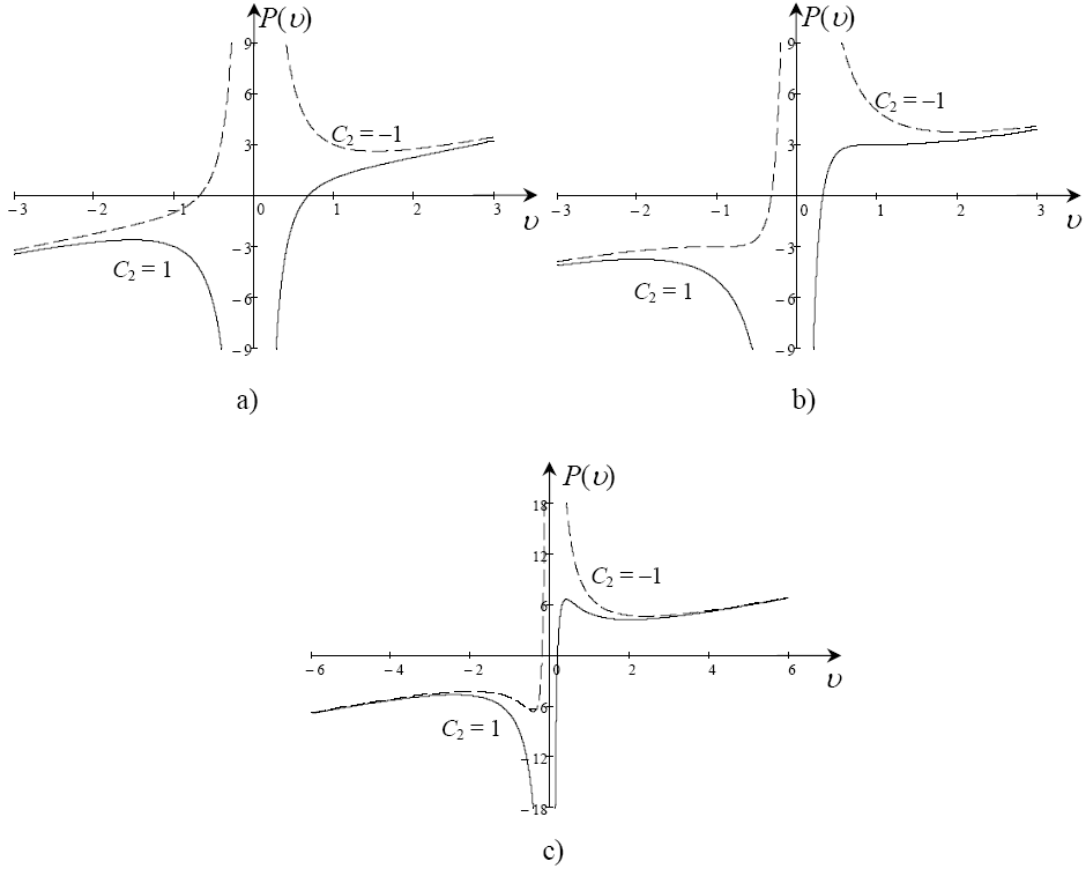
Figure 17. Potential function for the case $p + q \neq 0$. a) Supercritical case: $C_1 = -1$ and two values of C_2: $C_2 = 1$ (solid lines), and $C_2 = -1$ (dashed lines); b) marginal case: $C_1 = -3$ and the same two values of C_2; c) subcritical case: $C_1 = -5$ and the same two values of C_2 (in the last case the horizontal and vertical scales are doubled).

For the case of $C_2 = -1$ bounded solutions are smooth periodic waves which correspond to the particle oscillations in the potential well shown in the first quadrant in Fig. 15. Energy is positive for such motion and varies from $P_{\min} = 3(-C_2/4)^{1/3}$, where $P_{\min}$ is the local minimum of the right branch of the potential function (see Fig. 15) to infinity. Analytical solution for such waves can be also expressed in terms of cumbersome elliptic functions. Corresponding phase plane is presented in Fig. 16b.

4c. Consider now the case when both $C_1 \neq 0$ and $C_2 \neq 0$. The shape of the potential function is more complex in this case in general and depends on the relationship between the constants C_1 and C_2. The number and values of the potential extrema are determined by the number of real roots of the equation $P'(v) = 0$, where prime denotes the derivative on v. This condition yields (see equation (18)):

$$v^3 + C_1 v + 2C_2 = 0.$$

For real constants C_1 and C_2 this equation always has at least one real root. The real root is single when $C_1 \geq C_1^{\mathrm{cr}} \equiv -3C_2^{2/3}$; its value is given by the expression

$$v = \left[\sqrt{(C_1/3)^3 + C_2^2} - C_2 \right]^{1/3} - (C_1/3)\left[\sqrt{(C_1/3)^3 + C_2^2} - C_2 \right]^{-1/3}.$$

For the case $C_1 > C_1^{\mathrm{cr}}$, possible qualitative configurations of the potential function are shown in Fig. 17a for the particular choices of constants: $C_1 = -1$ and $C_2 = \pm 1$. There is only one
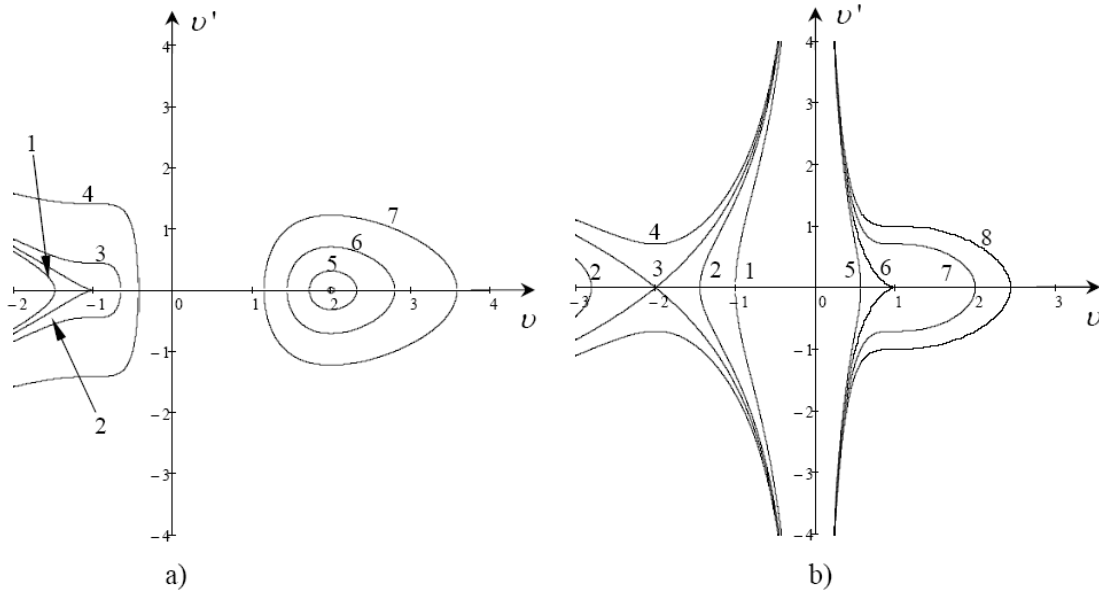
Figure 18. Phase plane corresponding to the marginal case, $C_1 = C_1^{\text{cr}}$. a) $C_1 = -3$, $C_2 = -1$. Line 1: $E = -3.05$; line 2: $E = -3$; line 3: $E = -2.9$; line 4: $E = -2$; line 5: $E = 3.8$; line 6: $E = 4$; line 7: $E = 4.5$. All trajectories in the left half-plane correspond to unbounded solutions. b) $C_1 = -3$, $C_2 = 1$. Line 1: $E = -5$; lines 2: $E = -4$; lines 3: $E = -3.75$; lines 4: $E = -3.5$; line 5: $E = 2.75$; line 6: $E = 3$; line 7: $E = 3.25$; line 8: $E = 3.5$.

local minimum at the right branch of the potential function for $C_2 = -1$ and a local maximum at the left branch of the potential function for $C_2 = 1$. Almost the same configuration of the potential function occurs for the marginal case $C_1 = C_1^{\text{cr}}$, as shown in Fig. 17b, however one more local extremum appears – on the left branch when $C_2 = -1$ and on the right branch when $C_2 = 1$. In the case $C_1 < C_1^{\text{cr}}$ the potential function is shown in Fig. 17c; there are three local extrema of the potential function for any value of $C_2 = \pm 1$.

The potential configuration in the supercritical case $C_1 > C_1^{\text{cr}}$ qualitatively is similar to the case shown in Fig. 15, therefore the corresponding phase portraits are similar to those shown in Fig. 16. In the marginal case, $C_1 = C_1^{\text{cr}}$, the potential configuration is also similar to those two cases mentioned above, however there are some peculiarities in the phase planes reflecting the appearance of embryos of new equilibrium points. Corresponding phase portraits are shown in Fig. 18. The embryos appear in the vicinity of $E = -3$ in Fig. 18a and in the vicinity of $E = 3$ in Fig. 18b.

In the subcritical case $C_1 < C_1^{\text{cr}}$ the situation is different from the previous ones and should be considered separately. In the case of $C_2 = -1$, there are two potential wells, one of a finite depth on the left branch of function $P(v)$ and another infinitely deep and wide well but bounded from the bottom on the right branch of function $P(v)$ (see Fig. 17c).

For the first potential well there is a family of closed trajectories in the phase plane corresponding to periodic solutions with the parameter E varying between the local minimum and maximum of the potential function; these solutions are described by elliptic functions. All closed trajectories are bounded by the loop of separatrix designated by symbol 3 in Fig. 19a. Trajectories inside the separatrix loop next to center correspond to quasi-sinusoidal waves, and the loop of the separatrix corresponds to the solitary wave (soliton) which can be treated as the limiting case of periodic waves. The soliton shape is described by the following implicit formula:

$$\eta = \pm\sqrt{2}\left[\frac{v_1}{2\sqrt{v_2 - v_1}}\ln\left(\frac{\sqrt{v_2 - v_1} + \sqrt{v_2 - v}}{\sqrt{v_2 - v_1} - \sqrt{v_2 - v}}\right) + \sqrt{v_2 - v}\right], \qquad v_1 \leq v \leq v_2, \tag{19}$$
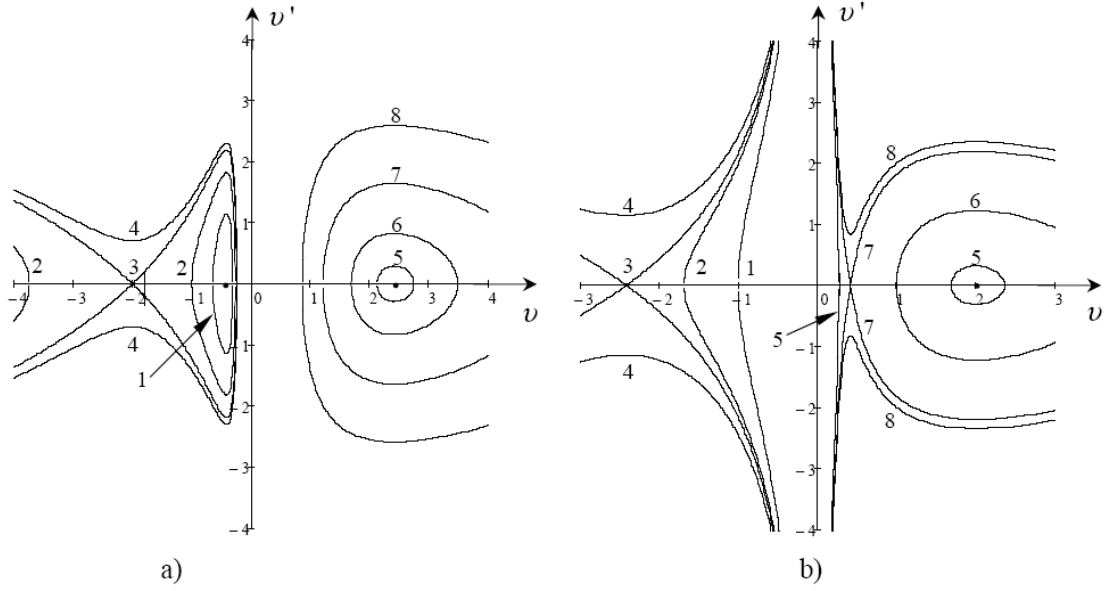
Figure 19. Phase plane corresponding to the subcritical case $C_1 < C_1^{\text{cr}}$. a) $C_1 = -5$, $C_2 = -1$. Line 1: $E = -6$; lines 2: $E = -5$; line 3: $E = -4.25$; lines 4: $E = -4$; line 5: $E = 4.7$; line 6: $E = 5$; line 7: $E = 6$; line 8: $E = 8$. All trajectories in the left half-plane outside of the closed loop of separatrix correspond to unbounded solutions. b) $C_1 = -5$, $C_2 = 1$. Line 1: $E = -7$; line 2: $E = -5$; lines 3: $E = -4.657$; lines 4: $E = -4$; line 5: $E = 4.3$; line 6: $E = 5$; lines 7: $E = 6.656$; lines 8: $E = 7$.
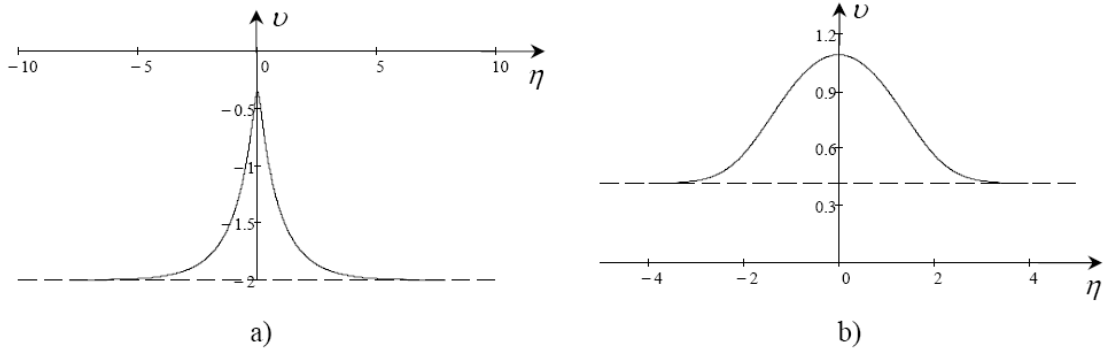

Figure 20. Soliton solutions on pedestals as described by equations (19).

where $v_{1,2} = -\left(C_1 \mp \sqrt{C_1^2 - 3EC_2}\right)/E$, $(v_1 < v_2)$ and $E = P_{\max}(C_1, C_2)$, where $P_{\max}(C_1, C_2)$ is the value of the potential local maximum shown in the left half-plane of Fig. 17c. Solution (19) is shown in Fig. 20a.

In original variables function u describing soliton varies in the range

$$V + \frac{6v_1}{p+q} \leq u \leq V + \frac{6v_2}{p+q};$$

thus, the soliton amplitude amounts

$$A = 6\frac{v_2 - v_1}{p+q} = \frac{12}{p+q}\frac{\sqrt{C_1^2 - 3C_2 P_{\max}(C_1, C_2)}}{P_{\max}(C_1, C_2)}; \tag{20}$$

The soliton velocity is

$$V = -\frac{1}{p}\left[\beta + 2P_{\max}(C_1, C_2)\right]. \tag{21}$$

Equations (20) and (21) allow one to obtain a direct relationship between the soliton's velocity and amplitude:

$$A = -\frac{24}{p+q} \frac{\sqrt{C_1^2 + \frac{3}{2}C_2(pV + \beta)}}{pV + \beta}.$$

For the second potential well located in the right half-plane of Fig. 17c, there is another family of closed trajectories in the phase plane corresponding to periodic solutions with the parameter E varying between the local minimum of the potential function and infinity; these trajectories are shown in the right half-plane of Fig. 19a.

In the case of $C_2 = 1$, there is a shallow potential well on the right branch of function $P(v)$ and one infinitely deep well at the origin where the potential function is singular. For the shallow well there is a family of closed trajectories in the phase plane corresponding to periodic solutions with the parameter E varying between the local minimum and maximum of the potential function. All such trajectories are also bounded by the loop of separatrix designated by symbol 7 in Fig. 19b. The loop of separatrix corresponds to the solitary wave whose shape is described by the same implicit formula (19), but with different values of constants C_1, C_2, E and $P_{\max}(C_1, C_2)$, where $P_{\max}(C_1, C_2)$ is the value of the potential local maximum shown in the right half-plane of Fig. 17c. This solution is shown in Fig. 20b. All above relationships between soliton amplitude and velocity, as well as between soliton amplitude or velocity and constants C_1 and C_2 remain the same as above.

For the infinitely deep well at the origin there are two families of compactons with nonpositive and nonnegative values; the phase plane for them is similar to that shown in Fig. 8 and solutions are similar to those shown in Fig. 9. The entire phase portrait of the system in the case of $C_2 = 1$ is shown in Fig. 19b. Phase trajectories corresponding to positive compactons are not shown in detail in that figure because they are too close to each other and are in the narrow gap between the axis v' and external two unclosed branches of the separatix 7 (only one such trajectory, line 5, is shown in Fig. 19b; all other trajectories are similar).

5   Conclusion

As was shown in the paper, the extended reduced Ostrovsky equation (1) possesses periodic and solitary type solutions in general. There is a variety of solitary-wave solutions including compactons with infinite derivatives at the edges, smooth solitons, and periodic waves. All compactons, however, actually are of the compound-type solutions, i.e., they consist of two or more non-smooth branches. Among periodic waves depending on the equation parameters, there are also both smooth solutions and compound-type solutions which consist of periodic sequences of non-smooth branches (see, e.g., Fig. 5b). Moreover, using compacton solutions as the elementary blocks, one can construct very complex compound solutions including stochastic stationary waves.

The approach used in this paper and based on the qualitative theory of dynamical systems is free from the limitations of paper [1] and allows us to present a complete classification of all possible solutions of stationary exROE. In particular, solutions were obtained and analyzed in details for the case $p + q = 0$ that was out of consideration in paper [1]. Another "prohibited" combination of parameters, $qV - \beta \neq 0$, that was also out of consideration in paper [1], does not even appear in our study. The approach exploited in the present paper is based on a vivid mechanical analogy between a particle moving in a special potential field and considered stationary exROE. This approach allows one to observe qualitatively an entire family of all possible solutions even without construction of particular exact solution. A similar approach has been exploited recently in application to the reduced Ostrovsky equation [4, 3] and exROE [3], although in the last case, the complete solution classification was not considered.

References

[1] Parkes E.J., Periodic and solitary travelling-wave solutions of an extended reduced Ostrovsky equation, *SIGMA* **4** (2008), 053, 17 pages, arXiv:0806.3155.

[2] Morrison A.J., Parkes E.J., The N-soliton solution of the modified generalised Vakhnenko equation (a new nonlinear evolution equation), *Chaos Solitons Fractals* **16** (2003), 13–26.

[3] Li J.-B., Dynamical understanding of loop soliton solution for several nonlinear wave equations, *Sci. China Ser. A* **50** (2007), 773–785.

[4] Stepanyants Y.A., On stationary solutions of the reduced Ostrovsky equation: Periodic waves, compactons and compound solitons, *Chaos Solitons Fractals* **28** (2006), 193–204.

[5] Ostrovsky L.A., Nonlinear internal waves in a rotating ocean, *Okeanologiya* **18** (1978), 181–191 (Engl. transl: *Oceanology* **18** (1978), 119–125).